SELF-PROPULSION ESTIMATIONS FOR A BULK CARRIER

Metin Kemal GOKCE[1, 3], Omer Kemal KINACI[2, *], Ahmet Dursun ALKAN[1]

[1] Naval Architecture and Maritime Faculty, Yildiz Technical University
[2] Faculty of Naval Architecture and Ocean Engineering, Istanbul Technical University
[3] Ceyhan Engineering Faculty, Cukurova University

Corresponding author e-mail: kinacio@itu.edu.tr

Abstract

Self-propulsion predictions are important to understand propeller-hull interactions and therefore the interaction between the main engine and the propulsion system. Experimental work encapsulates the core of self-propulsion estimations but due to their high cost, initial calculations are made using empirical relations suggested by the International Maritime Organization (IMO). However; these empirical relations may, at times, fail predicting some of the self-propulsion parameters. In this study, a specific example was chosen in which the IMO recommendations fail to predict the wake fraction. Numerical results utilizing RANSE are used to solve for the hull-propeller system to assess their validity in contrast with the experiments. RANSE is implemented in two different methods. The first one is by simulating directly the hull-propeller system while the second is the hull-virtual disk system, in which the propeller is only modelled as a circular disk without taking into account its geometry. Obtained results are discussed comparing them with the experiments and it was found out that numerical results are more robust with respect to empirical relations advised by the IMO.

Keywords: Japanese Bulk Carrier, JBC, thrust identity, virtual disk, self-propulsion, wake fraction

1. Introduction

Due to the high cost of experiments and time consuming processes of numerical studies, empirical relations still find common ground; especially by the engineers at the pre-design stages of a ship. Some of these empirical relations are also suggested by IMO or ITTC committees for the quick estimations of its various aspects.

Like all the other hydrodynamic properties, self-propulsion predictions may also rely on these basic empirical relations. Self-propulsion actually covers a complex interaction between the ship hull and the propeller but this interaction is roughly analyzed by two parameters; namely the wake fraction and the thrust deduction factor. Using these two parameters, the complex flow around the ship in whole is linearized and this linearization leads to making some predictions about the self-propulsion estimates. However, unusual or counter examples are always present; which force the shipbuilding industry to approach the problem in a more complex way. One of the most preferred methods is to adopt a computational strategy which is usually based on the application of Reynolds-averaged Navier-Stokes Equations (RANSE) based methods.

The benchmark Japanese Bulk Carrier (JBC) is one of these counter examples. The vessel has a bluff form that has high block coefficient and the recommendations of IMO to predict the wake fraction and the thrust deduction factor fail in estimating these interaction parameters. Therefore, in this study, a

RANSE-based Computational Fluid Dynamics (CFD) method was adopted to predict the self-propulsion point and discuss the effectiveness of IMO recommendations on inconvenient forms such as JBC.

Self-propulsion prediction of JBC was included in the Tokyo 2015 Workshop on CFD in Ship Hydrodynamics. Numerical results derived from 13 submissions from different organizations in the world were published in their website (T2015 Workshop). Cases were identified prior to the conference and all submissions were evaluated with respect to their selection of numerical approaches, number of elements in the domain etc. In this study, case 1.5 was simulated which involved self-propulsion in calm water with the propeller and without the rudder and ESD.

Other than this workshop, the current literature is short of studies on this specific benchmark ship. Wackers, Guilmineau and Visonneau (2017) investigated the unsteady behavior of RANS simulations using adaptive grid refinement. Another study by the same group mentions the difficulty of numerical flow prediction of JBC (Queutey, 2016). The local flow close to the propeller was examined numerically in their study and they have concluded that the flow around JBC was difficult to predict due to the unsteady behavior of a vortex structure at the stern part of the ship.

The rest of the paper was organized as follows: the general methodology to approximate the self-propulsion estimates of the ship using IMO recommendations was explained first. Then results using different numerical approaches with RANSE based CFD were presented. The numerical approach was tested with a verification and validation procedure to identify level of uncertainty in simulations. Finally, the results of basic approximation and CFD were compared with respect to experiment in terms of self-propulsion estimates.

2. Methodology

Self-propulsion estimations are usually made in towing tanks or numerical simulations including both the hull and the propeller. However; when the four components

- bare hull total resistance,
- open-water propeller performance,
- nominal wake fraction and
- thrust deduction factor

are known for a hull-propeller system, the self-propulsion estimates can closely be approximated by hand without the need for numerical or experimental results. The method generally consists of following steps;

1) Measure the bare hull total resistance R_T.
2) Obtain thrust coefficient K_T, torque coefficient K_Q and open-water propeller efficiency η_0 against advance coefficient J from open-water propeller tests.
3) Estimate nominal wake fraction w and thrust deduction t using IMO recommendations (IMO, 2013).
4) Experiments are usually conducted at model scale; therefore, calculate the skin friction correction (SFC) of the model using ITTC recommendations (ITTC, 7.5-02-03-01.4).
5) Calculate the required thrust using the equation

$$T = \frac{R_T - SFC}{1 - t} \tag{1}$$

6) Using the open-water propeller performance curve, obtain J, K_T, K_Q and η_0 at the theoretical self-propulsion point of the vessel.

All the other three, except the thrust deduction factor t, can be found from either bare hull or open-water propeller cases. On the other hand, the thrust deduction factor can be estimated by simulation of the hull-propeller system which requires a notable computational time. Therefore, a fast simplified approach is to make use of the empirical relations that may be found in the literature which consists of the 3rd step given above. The order of error of the self-propulsion approximation using the above methodology depends on how accurate the nominal wake fraction and the thrust deduction are predicted with the recommendations. The methodology along with some results based on this approach can be found in (Kinaci et al., 2018).

In this study, a specific example which does not obey the IMO recommendations was selected and its self-propulsion point was predicted by numerical simulations. The Japanese Bulk Carrier has a very high nominal wake fraction and thrust deduction factor which makes it hard to find its self-propulsion point using simple engineering relations.

3. Numerical implementation

Computational study in this work was carried out using a commercial software (Star CCM+) implementing RANSE and they can be classified into three parts. They are summarized as follows:

- bare hull numerical simulations which only take into account the hull,
- open-water propeller simulations which only take into account the propeller,
- self-propulsion simulations which both take into account the hull and the propeller.

Self-propulsion simulations can further be divided into two; using virtual disk to model the propeller and direct modeling of the propeller as a self-propelled case. The general outline of the selections made in the computational work is given as highlights below.

All the simulations were steady state at a model scale of $\lambda = 1/40$. The fluid domains were chosen with respect to the recommendations of the ITTC (7.5-03-02-03). The propeller rotation was modeled by the moving reference frame (MRF) approach. This approach is a fair one when cavitation is not expected and the acoustic properties of the propeller are not of interest. A $k - \omega\ SST$ turbulence model was implemented to solve for the turbulent flow around the ship. $k - \omega\ SST$ model was preferred to $k - \epsilon$ because JBC has a well-rounded form having a high block coefficient. $k - \omega\ SST$ is a better choice for bluff bodies. Wall y+ values were kept within an acceptable range taking into account the selection of the turbulence model. For this, prism layers were used close to the hull (and/or the propeller). Volume of Fluid (VOF) model was used to track the free surface where applicable (open-water propeller simulations were single phase so VOF was not activated). A special attention was paid to the Kelvin wake field at the free surface to correctly visualize the wave pattern which is shown in figure 1. Fluid properties like water density or viscosity were adjusted to be the same as in the experiments. The details of the number of elements used in simulations are given in Table 1.

For open-water propeller and direct self-propulsion simulations, two regions were created as is also explicit in Table 1. The propeller is surrounded by the rotating region and an interface surface was defined between the stationary and rotating regions. Stationary region is geometrically bigger but the rotating region has a denser mesh due to high pressure gradient expectation close to the propeller. Grid system used in these regions can be seen in Figure 2 for open-water propeller simulations and Figure 3 for the direct self-propulsion case with the propeller.

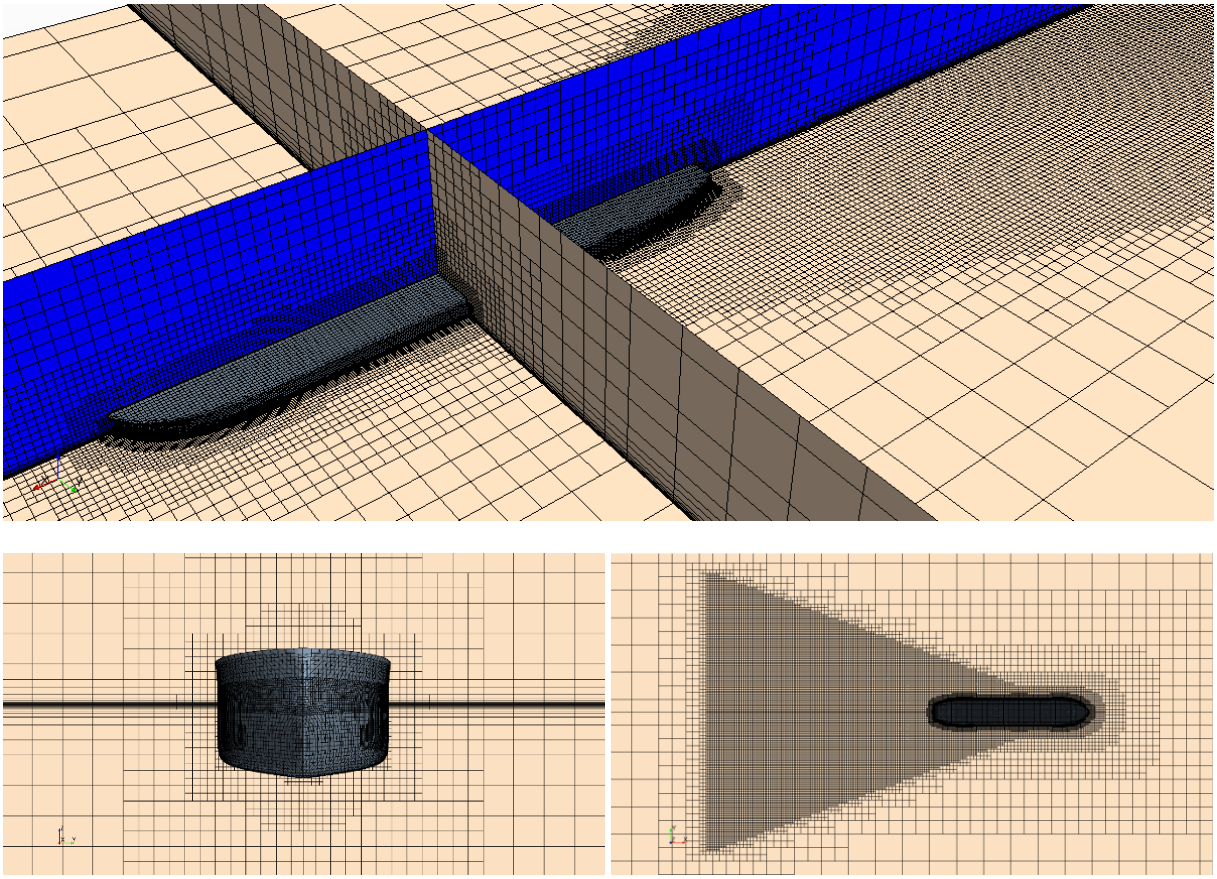

Figure 1. Some screenshots of the grid system around JBC (coarse grid). Number of elements was increased in places where Kelvin wake pattern was expected for better simulation of the free surface.

Table 1. Number of elements used in different simulations carried out in this study.

Type of numerical simulation	Number of elements		
	Stationary region	Rotating region	Total
Bare hull	2100k	-	2100k
Open-water propeller	600k	1200k	1800k
Self-propulsion using virtual disk	2520k	-	2520k
Direct self propulsion with propeller	2480k	1360k	3840k

Self-propulsion simulations were carried out in two different methods as also mentioned at the beginning of this section. The first was carried out without modeling the propeller but defining a virtual disk to represent the missing propeller. There is no rotating region in this type of simulation. The virtual disk was defined at the center of the propeller and had the same diameter of the original propeller.

Self-propulsion using virtual disk can be carried out with the grid system used in bare hull simulations. However; in this study, additional refinements were made close to the propeller region when implementing the virtual disk method to guarantee that the interaction between the hull and the propeller was better modelled.

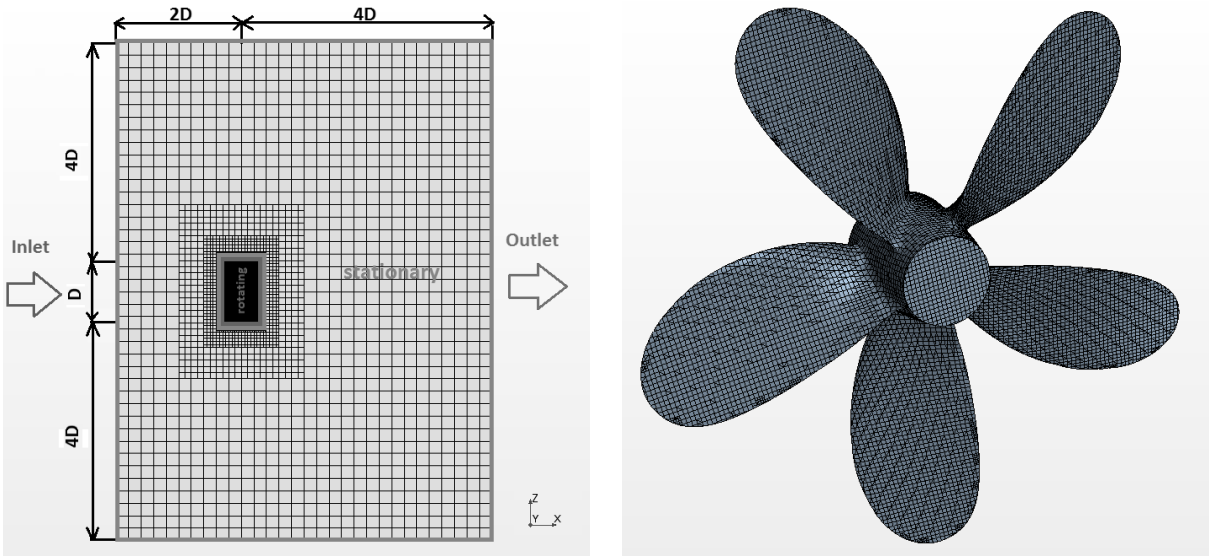

Figure 2. Grids used in the open-water propeller simulations. Fluid domain and the boundary conditions (left). A distance of 4D to the sides is present along y direction. JBC propeller (right).

The second self-propulsion simulation was the direct self-propulsion simulation with the propeller (ITTC, 7.5-03-03-01). The propeller was subtracted from a region enclosing it and was positioned at its correct location on JBC as given in Figure 3. The propeller was given an initial rotation and the rotation rate was adjusted to reach self-propulsion equilibrium.

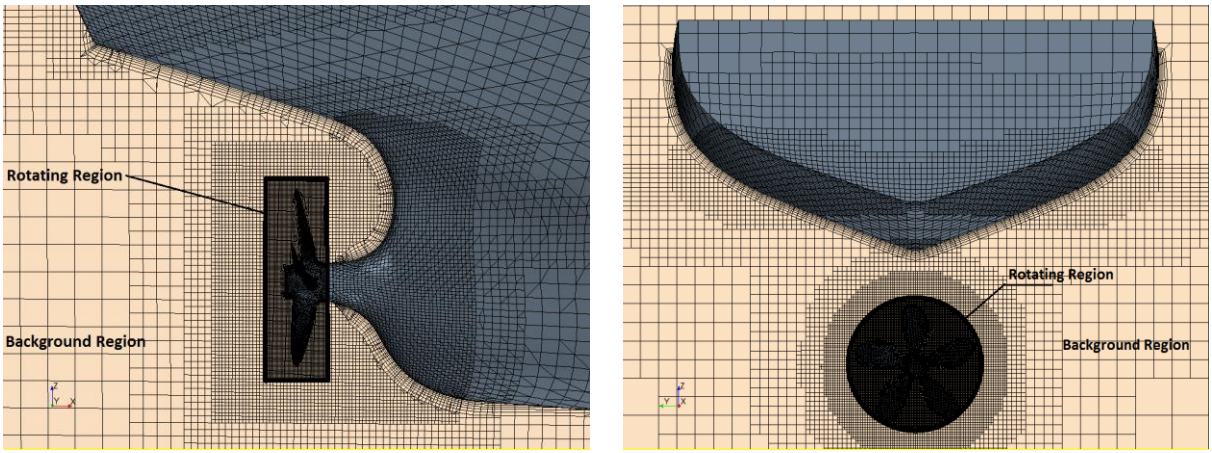

Figure 3. Grid system used in self-propelled CFD case. Refinements at the stern region are clearly visible. A view of background and rotating regions are also given.

4. Using a virtual disk approach to estimate self-propulsion

Bare hull simulations can provide useful data to predict the self-propulsion point of a vessel. Established methods which take into account the interactions between the propeller and the hull may be referred to estimate the details about the propulsion system like propulsion efficiencies such as η_H, η_R or the effective power, P_E. However; for the assessment of the interaction between the hull and the propeller, there is also a need for the open-water propeller performance.

Unlike the direct method in dealing with the self-propelled case, there are indirect ways to approach the self-propulsion problem of a ship. In these methods; nominal wake fraction w and total resistance R_T are obtained from experiments or numerical simulations of the bare hull. Propeller performance is determined from open-water tests (or simulations) and the self-propulsion point of the ship is identified by the thrust (or in some cases torque) identity method. In this section, the self-propulsion point of JBC was determined by the virtual disk method. Numerical simulations were performed for the bare hull and the open-water propeller cases and presented respectively; in comparison with the existing experiments found in the literature. The interaction between the two was studied at the end of the section using the virtual disk to model the propeller.

4.1. Numerical simulations for the bare hull

The test data, geometry and conditions for the JBC model are present at the website of the Tokyo 2015 Workshop on CFD in Ship Hydrodynamics. Main dimensions of the JBC model are provided in Table 2.

Table 2. Main dimensions of the bare hull JBC at model scale $\lambda = 1/40$.

Length between perpendiculars	L_{pp}	m	7
Waterline beam	B_{wl}	m	1.125
Draft	T	m	0.4125
Wetted surface area w/o the rudder	S	m^2	12.22
Block coefficient	C_B	-	0.858
Mid-ship section coefficient	C_M	-	0.9981
Service speed	V_m	m/s	1.179

The total resistance coefficient and the nominal wake fraction calculated by the numerical simulations are compared with the existing experimental data. Nominal wake fraction was calculated by the formula,

$$w = \frac{V_m - V_A}{V_m} \tag{2}$$

where V_m is the velocity of the ship model and V_A is the mean axial velocity received by the propeller. The total resistance coefficient was calculated by,

$$C_T = \frac{2R_T}{\rho S {V_m}^2} \tag{3}$$

Table 3. Bare hull numerical results in comparison with experiments.

	$C_T * 10^3$	w_{av}
Experiments	4.289	0.641
CFD	4.128	0.631
Error %	$3.75\%D$	$1.56\%D$

Using these two equations, the numerical results in comparison with the experiments at the service speed ($Fr = 0.142$) are given in Table 3. w_{av} in the table is calculated by adding up all w values at each grid A_g in the propeller disk and dividing it by the propeller disk area A_{pd} which is mathematically given by,

$$w_{av} = \frac{\sum w A_g}{A_{pd}} \tag{4}$$

Numerical bare hull simulations show good agreement with experiments in terms of the total resistance and the average nominal wake fraction. Comparison of the axial velocity that the propeller receives is given in Figure 4.

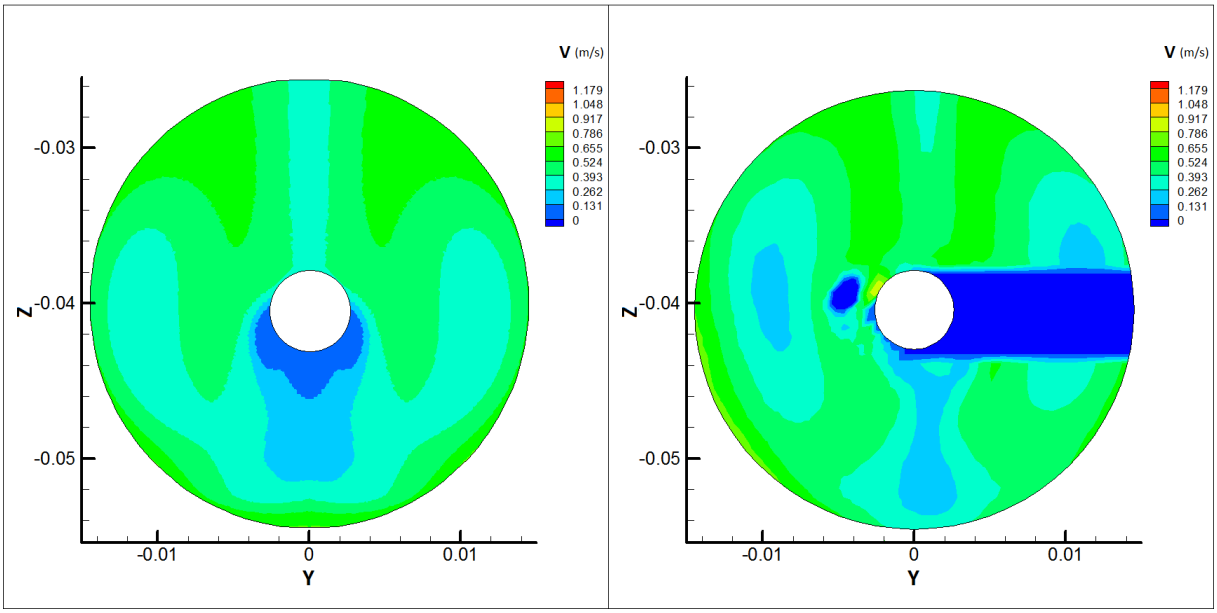

Figure 4. Axial velocity on the propeller disk derived from bare hull simulations (left). Experimental axial velocity on the propeller disk (right).

4.2. Open-water propeller performance

Open-water propeller performance of MP687 which is the original propeller of JBC was numerically simulated between the range $0.1 < J < 0.8$. Main properties of the propeller are given in Table 4. The advance coefficient was changed by keeping the advance speed V_A constant and changing the propeller rotation rate n. The results are depicted in Figure 5.

Table 4. Main properties of the MP687 propeller.

Propeller diameter	0.203 m
Boss ratio	0.18
Pitch ratio	0.75
Expanded area ratio	0.5
Rake angle	5°
Number of blades	5
Direction of rotation	Clockwise

The numerical simulations generated slightly higher torque and slightly lower thrust. However, these small differences in forces and moments created by the propeller reflect as a noticeable difference in open-water propeller efficiency η_0. This difference in results is especially sound at higher advance coefficients. The discrepancy probably arises due to the JBC propeller having high aft rake. The selected turbulence model ($k-\omega\ SST$) remains incapable to resolve real flow properties because of a bluffer propeller form. More advanced models might be required to assess the open-water propeller performance.

Both of these results (numerical and experimental) can be used for the prediction of self-point estimates for JBC. In this study, experimental results were used. The numerical results presented in this section for the open-water case were merely used for the validation of the numerical method.

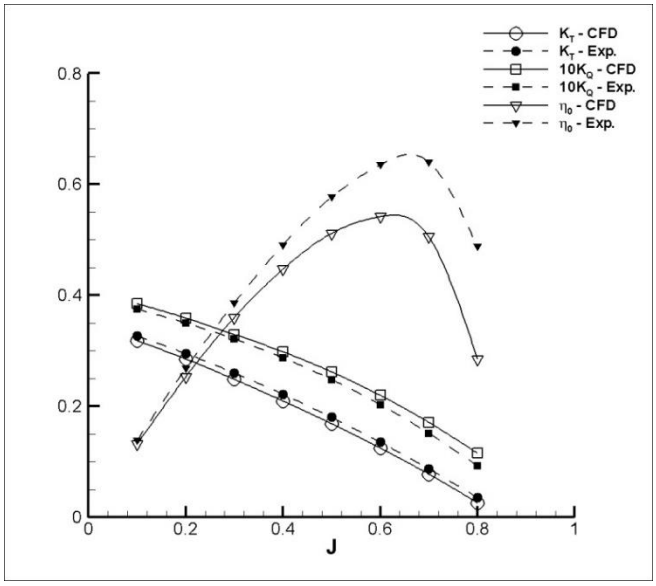

Figure 5. Numerically obtained open-water propeller performance graph and comparison with experimental data.

4.3. Virtual disk method

In this section; the geometry of the propeller was not modelled along with the hull but instead, it was modelled as a disk that uses its open-water performance. A recent example that utilizes this method is present in (Sezen et al., 2018). The self-propulsion estimates are calculated using the thrust identity approach following the recommendations of the (ITTC, 7.5-02-03-01.4). To make use of the thrust

identity approach for predicting all of the self-propulsion estimates, the thrust deduction factor should also be known. The thrust deduction factor t is calculated with the formula,

$$t = \frac{R_{T,sp} - R_{T,bh}}{R_{T,sp}} \tag{5}$$

$R_{T,sp}$ is the total resistance in self-propelled condition while $R_{T,bh}$ is the total resistance in bare hull condition. According to Equation (4), the total resistance of the self-propelled case has to be known a priori to calculate the thrust deduction. This situation poses a problem because there are two unknowns in Equation (5), t and $R_{T,sp}$. To overcome this problem, we have implemented a virtual disk method without modeling the propeller directly and using its open-water propeller results instead. This way, $R_{T,vd}$ is calculated instead of $R_{T,sp}$ and Equation (5) becomes,

$$t = \frac{R_{T,vd} - R_{T,bh}}{R_{T,vd}} \tag{6}$$

This approximation is considered to be a fair one as the virtual disk is approximating the effect of the propeller making use of its open-water performance. Using the virtual disk method, it was found out that the self-propulsion point of the model (taking into account the skin friction correction, $SFC = 18.2N$) was caught at $n = 8.09rps$ of the propeller and the total resistance at this self-propelled case was $C_{T,vd} = 4.54 * 10^{-3}$. The thrust deduction factor using Equation (6) was calculated to be $t = 0.091$. Summing up all the results given in sections 4.1, 4.2 and 4.3; the calculated self-propulsion estimates are given in Table 5. In that table, w_T is the Taylor wake fraction calculated by the thrust identity method and is given by the formula (ITTC, 7.5-03-03-01);

$$w_T = 1 - \frac{JnD}{V} \tag{7}$$

η_H is the hull efficiency and η_R is the relative-rotative efficiency which were calculated respectively by,

$$\eta_H = \frac{1 - t}{1 - w} \tag{8}$$

$$\eta_R = \frac{K_{Q_0}}{K_Q} \tag{9}$$

where K_{Q_0} denotes the torque coefficient in open water.

Table 5. Prediction of self-propulsion estimates using virtual disk.

	n	$C_T \cdot 10^3$	t	w_T	J	K_T	K_Q	η_0	η_H	η_R
Virtual Disk	8.09	4.54	0.091	0.669	0.48	0.184	0.0251	0.560	2.746	0.923

Results presented in Table 5 suggest a hull efficiency which is unexpectedly high for a conventional displacement ship. This is one of the drawbacks of the virtual disk method; as (Dogrul et al., 2018) have also encountered such a result. They have concluded in their study that the existence of the free water surface spoils the self-propulsion estimations. They state that such discrepancies do not exist in self-propulsion estimations for submarines.

5. A direct self-propelled CFD approach

A direct self-propelled numerical simulation including the geometry of the propeller was carried out for the completeness and the assessment of results. The CAD model of the propeller at is position on JBC is given in Figure 6. Predictions were made using the thrust identity method. Comparison of results with experiments and virtual disk are given in Table 6.

It should be stated that while calculating the self-propulsion estimates for the self-propelled CFD case, numerical results for the open-water propeller performance was used. The experimental results; however, depend on the experimental open-water propeller performance curve.

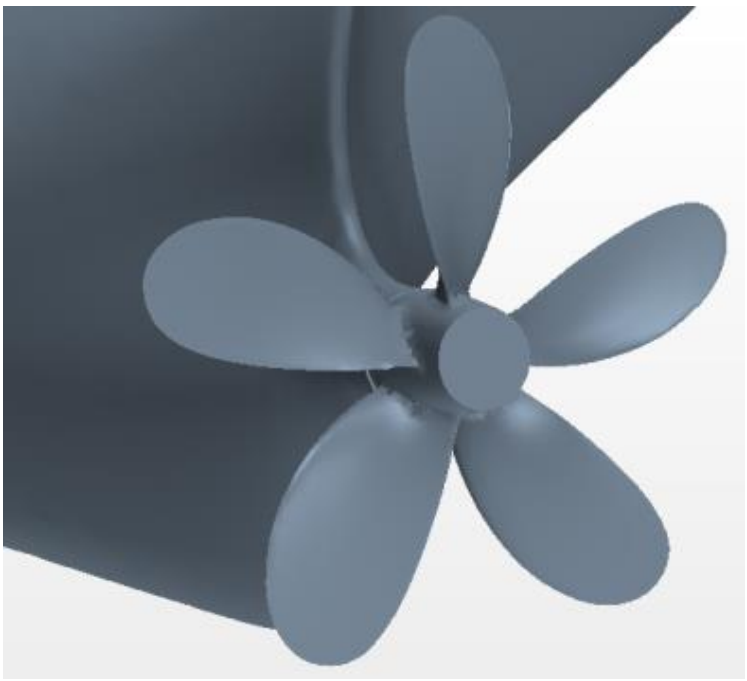

Figure 6. MP687 propeller in its position on JBC.

Table 6. Comparison of self-propulsion predictions.

	n	$C_T \cdot 10^3$	t	w_T	J	K_T	K_Q	η_0	η_H	η_R
Experiments	7.8	4.811	0.188	0.448	0.411	0.217	0.0279	0.501	1.471	1.015
Yin et al. (2015) *	7.68	4.607	0.069	0.473	0.398	0.223	0.0287	0.49	1.767	-
Schuiling et al. (2015) *	7.8	4.663	0.199	-	-	0.212	0.0251	-	-	-
Self-propelled CFD*	7.9	4.682	0.118	0.433	0.442	0.204	0.0285	0.473	1.556	0.977

* Using experimental open-water results.

Results depicted in Table 6 reveal that using a virtual disk to represent the propeller to estimate the self-propulsion condition of a vessel is unsatisfying. On the other hand, self-propelled CFD results are in good agreement with the experiments. Validation and verification study for the self-propelled CFD case is given in the next section.

A point that should be mentioned in this section is the better estimation of self-propulsion parameters of JBC compared to the open-water propeller simulations. It seems contradictory that the estimations are fair for the ship hull – propeller case when the numerical simulations for the propeller is 20% off

of the experiments at some specific advance ratios. The underlying reason is that the advance coefficient of self-propulsion case is $J = 0.442$ numerically; a point where the discrepancy between the numerical simulations and the experiments are comparably lower.

6. Verification and validation of the numerical study

A verification and validation (V&V) method for self-propelled numerical simulations was performed for JBC self-propulsion calculation with the methodology of (Stern et al., 2001). For the uncertainty assessment, self-propelled case simulations were used; therefore, rotational speed of the propeller at the self-propulsion point (n) was used as the integral variable. A similar uncertainty study using the rotation rate was made by (Korkmaz, 2015). Experimental results can be found in Tokyo 2015 CFD Workshop in Ship Hydrodynamics website and taken as the reference for uncertainty estimation of the numerical procedure. Skin friction correction was taken into account in calculations as per (ITTC, 7.5-02-03-01.4) Rotational speed of the propeller was changed during the simulations to get a difference of $18.2N$ (skin friction correction force) between self-propelled total resistance ($R_{T_{SP}}$) and propeller thrust (T).

All the simulations involved in this study were steady state and time step uncertainty is not applicable. Then, the total numerical uncertainty becomes,

$$U_N = \sqrt{{U_I}^2 + {U_G}^2} \tag{10}$$

The number of elements contained for each grid was increased with respect to Richardson extrapolation, $r_G = \sqrt{2}$. The rotational speeds at self-propulsion points using three different grid systems are given in Table 7, along with the iterative uncertainty for each grid.

Table 7. Estimation of rotation speeds for self-propulsion of JBC with different grids.

	Experiment (D)	GRID 1 (G_1)	GRID 2 (G_2)	GRID 3 (G_3)
no. of elements	-	11.4M	3.8M	1.3M
U_I	-	0.142	0.096	0.069
n (rps)	7.8	7.87	7.90	8.15

Verification parameters for numerical simulation uncertainty are given in Table 8. The meaning of these parameters can be found in the reference article (Stern et al., 2001). R_{G_2} was found to be 0.12 and lying between 0 and 1 which states that there is a monotonic convergence. The order of accuracy was found to be remarkably high, $p_G = 6.12$. $C_G = 7.338$ and it was considered that this value is sufficiently greater than 1. The total uncertainty of the second grid G_2 was found to be $6.1\%D$. Considering the uncertainties of rotational rates ranging between $4.78\%S$ to $26.06\%S$ in (Korkmaz, 2016), the level of uncertainty in this study was found to be fair.

Table 8. Verification parameters for numerical simulations.

ε_{32}	ε_{21}	R_{G_2}	r_G	p_G	δ_{RE}	C_G	U_G
0.25	0.03	0.12	1.414	6.12	0.0341	7.338	0.466

Validation parameters, which are identified in (Stern et al., 2001) for numerical simulation uncertainty, can be seen in Table 9. The experimental uncertainty is not provided in the workshop therefore the validation uncertainty is taken to be equal to the numerical uncertainty, $U_V \cong U_N$. Error for grid 2 was found to be $1.3\%D$. Comparison error was calculated by,

$$|E| = 100 * \frac{D - S}{D} \tag{11}$$

Validation uncertainty is equal to $U_V = 6.1\%D$ and comparison error $|E| < U_V$ states that the simulation results are validated.

Table 9. Validation parameters for numerical simulations.

Data (D)	Simulation (S_{G_2})	Error $\|E\|$
7.8 rps	7.9 rps	0.1 rps

7. Discussion

Results for the bare hull, open-water propeller, self-propulsion case using virtual disk and direct self-propelled case with the propeller itself were presented in the preceding sections along with a verification and validation of the numerical study. As is given in Table 2, JBC has a block coefficient of $C_B = 0.858$. IMO recommendations (2013) state that the nominal wake fraction is to be taken as $w = 0.35$ for vessels having $C_B > 0.8$. Again using IMO recommendations (2013), the thrust deduction factor is found to be $t = 0.245$. The comparison of these two results with the experimental values is given in Table 10.

Table 10. Nominal wake fraction and thrust deduction factor obtained with various methods.

IMO		Experiments	
w	t	w	t
0.35	0.245	0.641	0.109

It was observed that IMO largely fails in predicting the nominal wake fraction w and the thrust deduction factor t. Considering that these two parameters institute the core of the interaction between the hull and the propeller, it may be said that numerical results are more reliable when predicting the self-propulsion point of a vessel.

8. Conclusions

In this study; Japanese Bulk Carrier, which is an inconvenient hull form both for numerical and empirical predictions, was selected and its self-propulsion estimates were predicted. The difficulty in numerical flow predictions of this ship was also mentioned by other researchers in this field and in this work, it was shown that it is also difficult to estimate its flow properties by empirical relations. Still, it was found out that it is possible to generate better results using RANSE based methods. Quick estimations of self-propulsion by IMO recommendations are not possible for this specific ship as the interaction parameters such as the thrust deduction and nominal wake fraction are way off when compared with the experimental results.

Although slower than empirical methods, RANSE based methods offer good estimations of self-propulsion when the propeller is also modeled. It was found in this paper that the direct self-propelled CFD approach is superior to the body force propeller models such as the virtual disk method in determining the self-propulsion parameters. Direct modeling of the propeller provides a good approximation of these parameters especially when the self-propulsion advance coefficient is low. Open-water propeller simulations reveal that the relative errors compared to experiments are lower in low advance coefficients.

References

Dogrul A., Ozdemir Y. H., Sezen S. and Barlas B., 2018. Uncertainty assessment and self-propulsion estimation of Duisburg Test Case, 3rd International Symposium on Naval Architecture and Maritime, Turkey.

IMO Resolution MEPC.232(65). 2013 Interim guidelines for determining minimum propulsion. Power to maintain the manoeuverability of ships in adverse conditions, Annex 16.

ITTC 7.5-02-03-01.4:2014. Recommended procedures and guidelines. 1978 ITTC performance prediction method, revision 03.

ITTC 7.5-03-02-03:2014. Recommended procedures and guidelines. Practical guidelines for ship CFD applications, revision 01.

ITTC 7.5-03-03-01:2014. Recommended procedures and guidelines. Practical guidelines for ship self-propulsion CFD.

Kinaci O. K., Gokce, M. K., Alkan, A. D. and Kukner, A., 2018. On self-propulsion assessment of marine vehicles, Brodogradnja, 69(4), p. 29-51.

Korkmaz K. B., 2015. CFD predictions of resistance and propulsion for the JAPAN Bulk Carrier (JBC) with and without an energy saving device. Chalmers University of Technology, MSc. Thesis.

Queutey P., Guilmineau E., Visonneau M., Wackers J. and Deng G. B., 2016. RANS and hybrid RANS-LES simulations around the Japan Bulk Carrier of the Tokyo 2015 CFD Workshop, 19th Numerical Towing Tank Symposium, France.

Schuiling B., Windt J., Rijpkema D. R. and van Terwisga T. J. C., 2015. Computational study on power reduction by a pre-duct for a bulk carrier, Tokyo 2015 CFD Workshop, Japan.

Sezen S., Dogrul A., Delen C. and Bal S., 2018. Investigation of self-propulsion of DARPA Suboff by RANS method, Ocean Engineering, 150, p. 258-271.

Stern F., Wilson R. V., Coleman H. W. and Paterson E. G., 2001. Comprehensive approach to verification and validation of CFD simulations –Part 1: methodology and procedures, Journal of Fluids Engineering –Transactions of ASME, 123(4), p. 793-802.

T2015 Workshop. [online] Available at: http://www.t2015.nmri.go.jp [Accessed 7 Dec. 2017].

Wackers J., Guilmineau E. and Visonneau M., 2017. Unsteady behaviour in RANS simulation of the JBC and KVLCC2, 20th Numerical Towing Tank Symposium, Holland.

Yin C., Wu J., Sun T. and Wan D., 2015. A numerical study for self-propelled JBC with and without energy saving device, Tokyo 2015 CFD Workshop, Japan.

NOMENCLATURE

A_g	Area of the grid
A_{pd}	Propeller disk area
C_T	Total resistance coefficient
D	Propeller diameter
Fr	Froude number
J	Advance coefficient
K_T	Thrust coefficient
K_Q	Torque coefficient
n	Propeller rotation rate
P_E	Effective power
R_T	Total resistance
$R_{T,bh}$	Total resistance in bare hull condition
$R_{T,sp}$	Total resistance in self-propelled condition
$R_{T,vd}$	Total resistance with virtual disk
t	Thrust deduction factor
T	Thrust
U_G	Grid uncertainty
U_I	Iterative uncertainty
U_N	Total numerical uncertainty
V_A	Velocity received by the propeller
V_m	Velocity of the ship model
w	Nominal wake fraction
w_{av}	Average nominal wake fraction
w_T	Taylor wake fraction
η_0	Open-water propeller efficiency
η_H	Hull efficiency
η_R	Relative-rotative efficiency
ρ	Water density

ABBREVIATIONS

CAD	Computer aided design
CFD	Computational fluid dynamics
ESD	Energy saving device
IMO	International Maritime Organization
ITTC	International Towing Tank Conference
JBC	Japanese Bulk Carrier
MRF	Moving reference frame
RANSE	Reynolds-Averaged Navier-Stokes equations
SFC	Skin friction correction
SST	Shear stress transport
T2015	Tokyo 2015 CFD Workshop
VOF	Volume of fluid
V&V	Verification and validation